

# Fast Radix-10 Multiplication Using Redundant BCD Codes

Álvaro Vázquez, *Member, IEEE*, Elisardo Antelo, and Javier D. Bruguera, *Member, IEEE*

**Abstract**—We present the algorithm and architecture of a BCD parallel multiplier that exploits some properties of two different redundant BCD codes to speedup its computation: the redundant BCD excess-3 code (XS-3), and the overloaded BCD representation (ODDS). In addition, new techniques are developed to reduce significantly the latency and area of previous representative high-performance implementations. Partial products are generated in parallel using a signed-digit radix-10 recoding of the BCD multiplier with the digit set  $[-5, 5]$ , and a set of positive multiplicand multiples (0X, 1X, 2X, 3X, 4X, 5X) coded in XS-3. This encoding has several advantages. First, it is a self-complementing code, so that a negative multiplicand multiple can be obtained by just inverting the bits of the corresponding positive one. Also, the available redundancy allows a fast and simple generation of multiplicand multiples in a carry-free way. Finally, the partial products can be recoded to the ODDS representation by just adding a constant factor into the partial product reduction tree. Since the ODDS uses a similar 4-bit binary encoding as non-redundant BCD, conventional binary VLSI circuit techniques, such as binary carry-save adders and compressor trees, can be adapted efficiently to perform decimal operations. To show the advantages of our architecture, we have synthesized a RTL model for  $16 \times 16$ -digit and  $34 \times 34$ -digit multiplications and performed a comparative survey of the previous most representative designs. We show that the proposed decimal multiplier has an area improvement roughly in the range 20-35 percent for similar target delays with respect to the fastest implementation.

**Index Terms**—Parallel multiplication, decimal hardware, overloaded BCD representation, redundant excess-3 code, redundant arithmetic

## 1 INTRODUCTION

DECIMAL fixed-point and floating-point formats are important in financial, commercial, and user-oriented computing, where conversion and rounding errors that are inherent to floating-point binary representations cannot be tolerated [3]. The new IEEE 754-2008 Standard for Floating-Point Arithmetic [15], which contains a format and specification for decimal floating-point (DFP) arithmetic [1], [2], has encouraged a significant amount of research in decimal hardware [6], [9], [10], [28], [30].

Furthermore, current IBM Power and z/System families of microprocessors [5], [8], [23], and the Fujitsu Sparc X microprocessor [26], oriented to servers and mainframes, already include fully IEEE 754-2008 compliant decimal floating-point units (DFPUs) for Decimal64 (16 precision digits) and Decimal128 (34 precision digits) formats.

Since area and power dissipation are critical design factors in state-of-the-art DFPU, multiplication and division are performed iteratively by means of digit-by-digit

algorithms [4], [5], and therefore they present low performance. Moreover, the aggressive cycle time of these processors puts an additional constraint on the use of parallel techniques [6], [19], [30] for reducing the latency of DFP multiplication in high-performance DFPU. Thus, efficient algorithms for accelerating DFP multiplication should result in regular VLSI layouts that allow an aggressive pipelining.

Hardware implementations normally use BCD instead of binary to manipulate decimal fixed-point operands and integer significands of DFP numbers for easy conversion between machine and user representations [21], [25]. BCD encodes a number  $X$  in decimal (non-redundant radix-10) format, with each decimal digit  $X_i \in [0, 9]$  represented in a 4-bit binary number system. However, BCD is less efficient for encoding integers than binary, since codes 10 to 15 are unused. Moreover, the implementation of BCD arithmetic has more complications than binary, which lead to area and delay penalties in the resulting arithmetic units.

A variety of redundant decimal formats and arithmetics have been proposed to improve the performance of BCD multiplication. The BCD carry-save format [9] represents a radix-10 operand using a BCD digit and a carry bit at each decimal position. It is intended for carry-free accumulation of BCD partial products using rows of BCD digit adders arranged in linear [9], [20] or tree-like configurations [19]. Decimal signed-digit (SD) representations [10], [14], [24], [27] rely on a redundant digit set  $\{-a, \dots, 0, \dots, a\}$ ,  $5 \leq a \leq 9$ , to allow decimal carry-free addition.

BCD carry-save and signed-digit radix-10 arithmetics offer improvements in performance with respect to non-redundant BCD. However, the resultant VLSI implementations in current technologies of multioperand adder trees may result in more irregular layouts than binary carry-save adders (CSA) and compressor trees.

- A. Vázquez is with the Centro de Investigación en Tecnologías de Información (CITIUS), University of Santiago de Compostela, 15782 Santiago de Compostela, Spain. E-mail: alvaro.vazquez@usc.es.
- E. Antelo is with the Department of Electrical and Computer Engineering, University of Santiago de Compostela, Spain. E-mail: elisardo.antelo@usc.es.
- J.D. Bruguera is with the Department of Electrical and Computer Engineering, University of Santiago de Compostela, Spain, and the Centro de Investigación en Tecnologías de Información (CITIUS), University of Santiago de Compostela, 15782 Santiago de Compostela, Spain. E-mail: jd.bruguera@usc.es.

Manuscript received 15 Sep. 2013; revised 13 Jan. 2014; accepted 5 Mar. 2014. Date of publication 3 Apr. 2014; date of current version 15 July 2014. Recommended for acceptance by A. Nannarelli, P.-M. Seidel, and P.T.P. Tang. For information on obtaining reprints of this article, please send e-mail to: reprints@ieee.org, and reference the Digital Object Identifier below. Digital Object Identifier no. 10.1109/TC.2014.2315626

Some approaches rely on binary arithmetic to perform decimal multioperand addition and multiplication. In [6], a decimal multioperand adder is implemented using columns of binary compressors and subsequent binary-to-BCD conversions. Also, decimal multioperand addition can be improved using binary carry-save adders and decimal doublers if digits are not represented in BCD but in certain decimal codes, namely, 4221 and 5211. These 4-bit decimal codes satisfy that the sum of the weights of the bits is equal to 9, so that all the 16 4-bit combinations represent a decimal digit in  $[0, 9]$ . These codes have been used to speed-up decimal multioperand addition and multiplication [29], [30], [31]. The additional redundancy available in the 4-bit encoding is used to speed-up BCD operations while retaining the same data path width.

Furthermore, these codes are self-complementing, so that the 9's complement of a digit, required for negation, is easily obtained by bit-inversion of its 4-bit representation. A disadvantage of 4221 and 5211 codes, is the use of a non-redundant radix-10 digit set  $[0, 9]$  as BCD. Thus, the redundancy is constrained to the digit bounds, so that complex decimal multiples, such as  $3X$ , cannot be obtained in a carry-free way.

The overloaded BCD (or ODDS—overloaded decimal digit set) representation was proposed to improve decimal multioperand addition [18], and sequential [17] and parallel [12], [13] decimal multiplications. In this code, each 4-bit binary value represents a redundant radix-10 digit  $X_i \in [0, 15]$ . The ODDS presents interesting properties for a fast and efficient hardware implementation of decimal arithmetic: (1) it is a redundant decimal representation so that it allows carry-free generation of both simple and complex decimal multiples ( $2X$ ,  $3X$ ,  $4X$ ,  $5X$ ,  $6X$ ,...) and addition, (2) since digits are represented in the binary number system, digit operations can be performed with binary arithmetic, and (3) unlike BCD, there is no need to implement additional hardware to correct invalid 4-bit combinations. A disadvantage with respect to signed-digit and self-complementing codes, is a slightly more complex implementation of 9's complement operation for negation of operands and subtraction.

In this work, we focus on the improvement of parallel decimal multiplication by exploiting the redundancy of two decimal representations: the ODDS and the redundant BCD excess-3 (XS-3) representation, a self-complementing code with the digit set  $[-3, 12]$ . We use a minimally redundant digit set for the recoding of the BCD multiplier digits, the signed-digit radix-10 recoding [30], that is, the recoded signed digits are in the set  $\{-5, -4, -3, -2, -1, 0, 1, 2, 3, 4, 5\}$ . For this digit set, the main issue is to perform the  $\times 3$  multiple without long carry-propagation (note that  $\times 2$  and  $\times 5$  are easy multiples for decimal [30] and that  $\times 4$  is generated as two consecutive  $\times 2$  operations). We propose the use of a general redundant BCD arithmetic (that includes the ODDS, XS-3 and BCD representations) to accelerate parallel BCD multiplication in two ways:

- *Partial product generation (PPG)*. By generating positive multiplicand multiples coded in XS-3 in a carry-free form. An advantage of the XS-3 representation over non-redundant decimal codes (BCD and 4221/

5211 [30]) is that all the interesting multiples for decimal partial product generation, including the  $3X$  multiple, can be implemented in constant time with an equivalent delay of about three XOR gate levels. Moreover, since XS-3 is a self-complementing code, the 9's complement of a positive multiple can be obtained by just inverting its bits as in binary.

- *Partial product reduction (PPR)*. By performing the reduction of partial products coded in ODDS via binary carry-save arithmetic. Partial products can be recoded from the XS-3 representation to the ODDS representation by just adding a constant factor into the partial product reduction tree. The resultant partial product reduction tree is implemented using regular structures of binary carry-save adders or compressors. The 4-bit binary encoding of ODDS operands allows a more efficient mapping of decimal algorithms into binary techniques. By contrast, signed-digit radix-10 and BCD carry-save redundant representations require specific radix-10 digit adders [14], [22], [27].

The paper is organized as follows. Section 2 introduces formally the redundant BCD representations used in this work. Section 3 outlines the high level implementation (algorithm and architecture) of the proposed BCD parallel multiplier. In Section 4 we describe the techniques developed for the generation of decimal partial products. Decimal partial product reduction and the final conversion to a non-redundant BCD product are detailed in Sections 5 and 6 respectively. In Section 7 we provide area and delay estimates and a comparison with other representative decimal implementations that show the potential advantages of our proposal. We finally summarize the main conclusions and contributions of this work in Section 8.

## 2 REDUNDANT BCD REPRESENTATIONS

The proposed decimal multiplier uses internally a redundant BCD arithmetic to speed up and simplify the implementation. This arithmetic deals with radix-10 ten's complement integers of the form:

$$Z = -s_z \times 10^d + \sum_{i=0}^{d-1} Z_i \times 10^i, \quad (1)$$

where  $d$  is the number of digits,  $s_z$  is the sign bit, and  $Z_i \in [l - e, m - e]$  is the  $i$ th digit, with

$$0 \leq l \leq e, \quad 9 + e \leq m \leq 2^4 - 1 (= 15).$$

Parameter  $e$  is the excess of the representation and usually takes values 0 (non excess), 3 or 6. The redundancy index  $\rho$  is defined as  $\rho = m - l + 1 - r$  [12], being  $r = 10$ .

The value of  $Z_i$  depends on the decimal representation parameterized by  $(l, m, e)$ . We use a 4-bit encoding to represent digits  $Z_i$ . This allows us to manage decimal operands in different representations with the same arithmetic, such as BCD ( $Z_i \in [0, 9]$ ,  $e = 0$ ,  $l = 0$ ,  $m = 9$ ,  $\rho = 0$ ), BCD excess-3 ( $Z_i \in [0, 9]$ ,  $e = 3$ ,  $l = 3$ ,  $m = 12$ ,  $\rho = 0$ ), BCD excess-6 ( $Z_i \in [0, 9]$ ,  $e = 6$ ,  $l = 6$ ,  $m = 15$ ,  $\rho = 0$ ), and redundant representations ( $\rho > 0$ ), such as the ODDS representation ( $Z_i \in [0, 15]$ ,  $e = 0$ ,  $l = 0$ ,  $m = 15$ ,  $\rho = 6$ ), or the XS-3 representation ( $Z_i \in [-3, 12]$ ,  $e = 3$ ,  $l = 0$ ,  $m = 15$ ,  $\rho = 6$ ).

On the other hand, the binary value of the 4-bit vector representation of  $Z_i$  is given by

$$[Z_i] = \sum_{j=0}^3 z_{i,j} \times 2^j, \quad (2)$$

$z_{i,j}$  being the  $j$ th bit of the  $i$ th digit. Therefore, the value of digit  $Z_i$  can be obtained by subtracting the excess  $e$  of the representation from the binary value of its 4-bit encoding, that is,

$$Z_i = [Z_i] - e.$$

Note that bit-weighted codes such as BCD and ODDS use the 4-bit binary encoding (or BCD encoding) defined in Expression (2). Thus,  $Z_i = [Z_i]$  for operands  $Z$  represented in BCD or ODDS.

This binary encoding simplifies the hardware implementation of decimal arithmetic units, since we can make use of state-of-the-art binary logic and binary arithmetic techniques to implement digit operations. In particular, the ODDS representation presents interesting properties (redundancy and binary encoding of its digit set) for a fast and efficient implementation of multioperand addition. Moreover, conversions from BCD to the ODDS representation are straightforward, since the digit set of BCD is a subset of the ODDS representation.

In our work we use a SD radix-10 recoding of the BCD multiplier [30], which requires to compute a set of decimal multiples ( $\{-5X, \dots, 0X, \dots, 5X\}$ ) of the BCD multiplicand. The main issue is to perform the  $\times 3$  multiple without long carry-propagation.

For input digits of the multiplicand in conventional BCD (i.e., in the range  $[0, 9]$ ,  $e = 0$ ,  $\rho = 0$ ), the multiplication by 3 leads to a maximum decimal carry to the next position of 2 and to a maximum value of the interim digit (the result digit before adding the carry from the lower position) of 9. Therefore the resultant maximum digit (after adding the decimal carry and the interim digit) is 11. Thus, the range of the digits after the  $\times 3$  multiplication is in the range  $[0, 11]$ . Therefore the redundant BCD representations can host the resultant digits with just one decimal carry propagation.

An important issue for this representation is the ten's complement operation. Since after the recoding of the multiplier digits, negative multiplication digits may result, it is necessary to negate (ten's complement) the multiplicand to obtain the negative partial products. This operation is usually done by computing the nine's complement of the multiplicand and adding a one in the proper place on the digit array.

The nine's complement of a positive decimal operand is given by

$$-10^d + \sum_{i=0}^{d-1} (9 - Z_i) \times 10^i. \quad (3)$$

The implementation of  $(9 - Z_i)$  leads to a complex implementation, since the  $Z_i$  digits of the multiples generated may take values higher than 9. A simple implementation is obtained by observing that the excess-3 of the nine's complement of an operand is equal to the bit-complement of the operand coded in excess-3.

TABLE 1  
Nine's Complement for the XS-3 Representation

Digit			Nine's Complement		
4-bit Encoding	$Z_i$	$[Z_i]$	4-bit Encoding	$9 - Z_i$	$[9 - Z_i]$ ( $=15 - [Z_i]$ )
0000	-3	0	1111	12	15
0001	-2	1	1110	11	14
0010	-1	2	1101	10	13
0011	0	3	1100	9	12
0100	1	4	1011	8	11
0101	2	5	1010	7	10
0110	3	6	1001	6	9
0111	4	7	1000	5	8
1000	5	8	0111	4	7
1001	6	9	0110	3	6
1010	7	10	0101	2	5
1011	8	11	0100	1	4
1100	9	12	0011	0	3
1101	10	13	0010	-1	2
1110	11	14	0001	-2	1
1111	12	15	0000	-3	0

In Table 1 we show how the nine's complement can be performed by simply inverting the bits of a digit  $Z_i$  coded in XS-3. At the decimal digit level, this is due to the fact that:

$$(9 - Z_i) + 3 = 15 - (Z_i + 3) \quad (4)$$

for the ranges  $Z_i \in [-3, 12]$  ( $[Z_i] \in [0, 15]$ ). Therefore to have a simple negation for partial product generation we produce the decimal multiples in an excess-3 code. The negation is performed by simple bit inversion, that corresponds to the excess-3 of the nine's complement of the multiple. Moreover, to simplify the implementation we combine the multiple generation stage and the digit increment by 3 (to produce the excess-3) into a single module by using the XS-3 code (more details in Section 4.1).

In summary, the main reasons for using the redundant XS-3 code are: (1) to avoid long carry-propagations in the generation of decimal positive multiplicand multiples, (2) to obtain the negative multiples from the corresponding positive ones easily, (3) simple conversion of the partial products generated in XS-3 to the ODDS representation for efficient partial product reduction (more details in Section 4.3).

### 3 HIGH-LEVEL ARCHITECTURE

The high-level block diagram of the proposed parallel architecture for  $d \times d$ -digit BCD decimal integer and fixed-point multiplication is shown in Fig. 1. This architecture accepts conventional (non-redundant) BCD inputs  $X, Y$ , generates redundant BCD partial products  $PP$ , and computes the BCD product  $P = X \times Y$ . It consists of the following three stages<sup>1</sup>: (1) parallel generation of partial products coded in XS-3, including generation of multiplicand multiples and recoding of the multiplier operand, (2) recoding of partial products from XS-3 to the ODDS representation and subsequent reduction, and (3) final conversion to a non-redundant  $2d$ -digit BCD product.

1. Each stage is explained in detail in the next sections, stage 1 in Section 4, stage 2 in Section 5, and stage 3 in Section 6. In particular, we provide implementations suited for the IEEE 754-2008 decimal arithmetic formats [15], that is, for  $d = 16$  (Decimal64) and  $d = 34$  digits (Decimal128) in Sections 5.1 and 5.2, respectively.

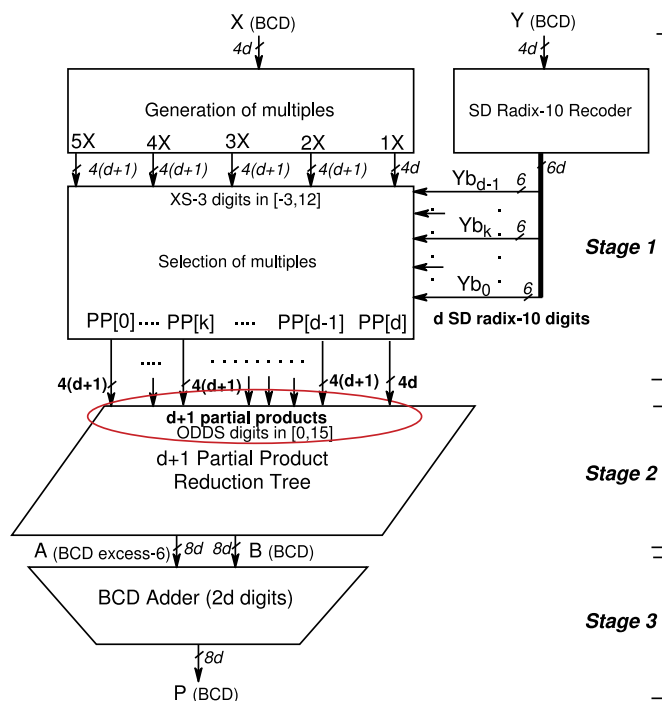


Fig. 1. Combinational SD radix-10 architecture.

*Stage 1) Decimal partial product generation.* A SD radix-10 recoding of the BCD multiplier has been used. This recoding produces a reduced number of partial products that leads to a significant reduction in the overall multiplier area [29]. Therefore, the recoding of the  $d$ -digit multiplier  $Y$  into SD radix-10 digits  $Yb_{d-1}, \dots, Yb_0$ , produces  $d$  partial products  $PP[d-1], \dots, PP[0]$ , one per digit; note that each  $Yb_k$  recoded digit is represented in a 6-bit hot-one code to be used as control input of the multiplexers for selecting the proper multiplicand multiple,  $\{-5X, \dots, -1X, 0X, 1X, \dots, 5X\}$ . An additional partial product  $PP[d]$  is produced by the most significant multiplier digit after the recoding, so that the total number of partial products generated is  $d+1$ .

In contrast to our previous SD radix-10 implementations [29], [30],  $3X$  is obtained in a reduced constant time delay ( $\approx 3$  XOR-gate delays) by using the XS-3 representation. Moreover, a negative multiple is generated from the correspondent positive one by a bitwise XOR operation. Consequently, the latency is reduced and the hardware implementation is simplified. The scheme proposed in [14] also produces  $3X$  in constant time but using redundant signed-digit BCD arithmetic.

*Stage 2) Decimal partial product reduction.* In this stage, the array of  $d+1$  ODDS partial products are reduced to two  $2d$ -digit words ( $A, B$ ). Our proposal relies on a binary carry-save adder tree to perform carry-free additions of the decimal partial products. The array of  $d+1$  ODDS partial products can be viewed as adjacent digit columns of height  $h \leq d+1$ . Since ODDS digits are encoded in binary, the rules for binary arithmetic apply within the digit bounds, and only carries generated between radix-10 digits (4-bit columns) contribute to the decimal correction of the binary sum. That is, if a carry out is produced as a result of a 4-bit (modulo 16) binary addition, the binary sum must be

incremented by 6 at the appropriate position to obtain the correct decimal sum (modulo 10 addition).

Two previous designs [12], [18] implement tree structures for the addition of ODDS operands. In the nonspeculative BCD adder [18], a combinational logic block is used to determine the sum correction after all the operands have been added in a binary CSA tree, with the maximum number of inputs limited to 19 BCD operands.<sup>2</sup> By contrast, in our method the sum correction is evaluated concurrently with the binary carry-save additions using columns of binary counters. Basically we count the number of carries per decimal column and then a multiplication by 6 is performed (a correction by 6 for each carry-out from each column). The result is added as a correction term to the output of the binary carry-save reduction tree. This improves significantly the latency of the partial product reduction tree. Moreover, the proposed architecture accepts an arbitrary number of ODDS or BCD operand inputs. Some of PPR tree structures presented in [12] (the area-improved PPR tree) also exploit a similar idea, but rely on a custom designed ODDS adder to perform some of the stage reductions. Our proposal aims to provide an optimal reuse of any binary CSA tree for multioperand decimal addition, as it was done in [31] for the 4221 and 5211 decimal codings.

*Stage 3) Conversion to (non-redundant) BCD.* We consider the use of a BCD carry-propagate adder [29] to perform the final conversion to a non-redundant BCD product  $P = A + B$ . The proposed architecture is a  $2d$ -digit hybrid parallel prefix/carry-select adder, the BCD Quaternary Tree adder (see Section 6). The sum of input digits  $A_i, B_i$  at each position  $i$  has to be in the range  $[0, 18]$  so that at most one decimal carry is propagated to the next position  $i+1$  [22]. Furthermore, to generate the correct decimal carry, the BCD addition algorithm implemented requires  $A_i + B_i$  to be obtained in excess-6. Several choices are possible. We opt for representing operand  $A$  in BCD excess-6 ( $A_i \in [0, 9], [A_i] = A_i + e, e = 6$ ), and  $B$  coded in BCD ( $B_i \in [0, 9], e = 0$ ).

## 4 DECIMAL PARTIAL PRODUCT GENERATION

The partial product generation stage comprises the recoding of the multiplier to a SD radix-10 representation, the calculation of the multiplicand multiples in XS-3 code and the generation of the ODDS partial products.

The SD radix-10 encoding produces  $d$  SD radix-10 digits  $Yb_k \in [-5, 5]$ , with  $k = 0, \dots, d-1$ ,  $Yb_{d-1}$  being the most significant digit (MSD) of the multiplier [29]. Each digit  $Yb_k$  is represented with a 5-bit hot-one code ( $Y1_k, Y2_k, Y3_k, Y4_k, Y5_k$ ) to select the appropriate multiple  $\{1X, \dots, 5X\}$  with a 5:1 mux and a sign bit  $Ys_k$  that controls the negation of the selected multiple.

The negative multiples are obtained by ten's complementing the positive ones. This is equivalent to taking the nine's complement of the positive multiple and then adding 1. As we have shown in Section 2, the nine's complement can be obtained simply by bit inversion. This needs

2. Providing support for 20 or more input BCD operands would require a significant modification of the original nonspeculative addition algorithm.

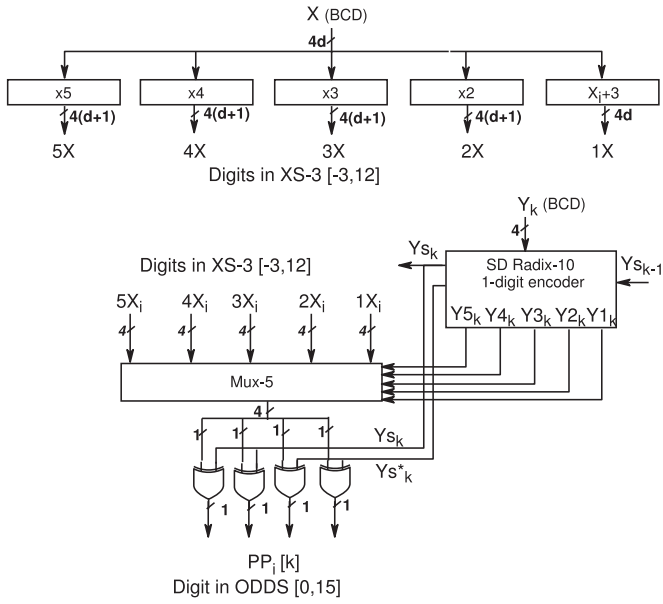


Fig. 2. SD radix-10 generation of a partial product digit.

the positive multiplicand multiples to be coded in XS-3, with digits in  $[-3, 12]$ .

The  $d$  least significant partial products  $PP[d-1], \dots, PP[0]$  are generated from digits  $Yb_k$  by using a set of 5:1 muxes, as shown in Fig. 2. The xor gates at the output of the mux invert the multiplicand multiple, to obtain its 9's complement, if the SD radix-10 digit is negative ( $Ys_k = 1$ ).

On the other hand, if the signals ( $Y1_k, Y2_k, Y3_k, Y4_k, Y5_k$ ) are all zero then  $PP[k] = 0$ , but it has to be coded in XS-3 (bit encoding 0011). Then, to set the two least significant bits to 1, the input to the XOR gate is  $Ys_k^* = Ys_k \vee Yb_{k-iszero}$  ( $\vee$  denotes the boolean OR operator), where  $Yb_{k-iszero}$  equals 1 if all the signals ( $Y1_k, Y2_k, Y3_k, Y4_k, Y5_k$ ) are zero.

In addition, the partial product signs are encoded into their MSDs (see Section 4.2). The generation of the most significant partial product  $PP[d]$  is described in Section 4.4, and only depends on  $Ys_{d-1}$ , the sign of the most significant SD radix-10 digit.

#### 4.1 Generation of the Multiplicand Multiples

We denote by  $NX \in \{1X, 2X, 3X, 4X, 5X\}$ , the set of multiplicand multiples coded in the XS-3 representation, with digits  $NX_i \in [-3, 12]$ , being  $[NX_i] = NX_i + 3 \in [0, 15]$  the corresponding value of the 4-bit binary encoding of  $NX_i$  given by Equation (2).

Fig. 3 shows the high-level block diagram of the multiples generation with just one carry propagation. This is performed in two steps:

1) digit recoding of the BCD multiplicand digits  $X_i$  into a decimal carry  $0 \leq T_i \leq T_{max}$  and a digit  $-3 \leq D_i \leq 12 - T_{max}$ , such as

$$D_i + 10 \times T_i = (N \times X_i) + 3, \quad (5)$$

being  $T_{max}$  the maximum possible value for the decimal carry.

2) The decimal carries transferred between adjacent digits are assimilated obtaining the correct 4-bit representation of XS-3 digits  $NX_i$ , that is

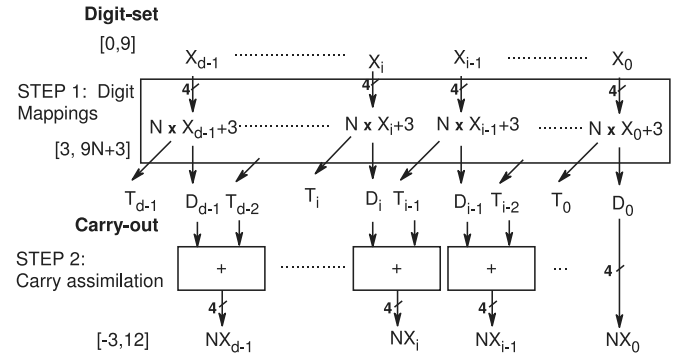


Fig. 3. Generation of a decimal multiples  $NX$ .

$$[NX_i] = D_i + T_{i-1}, [NX_i] \in [0, 15] (NX_i \in [-3, 12]). \quad (6)$$

The constraint for  $NX_i$  still allows different implementations for  $NX$ . For a specific implementation, the mappings for  $T_i$  and  $D_i$  have to be selected. Table 2 shows the preferred digit recoding for the multiples  $NX$ .

Then, by inverting the bits of the representation of  $NX$ , operation defined at the  $i$ th digit by

$$\overline{NX}_i = 15 - [NX_i],$$

we obtain  $\overline{NX}$ . Replacing the relation between  $NX_i$  and  $[NX_i]$  in the previous expression, it follows that

$$\overline{NX}_i = 15 - (NX_i + 3) = (9 - NX_i) + 3.$$

That is,  $\overline{NX}$  is the 9's complement of  $NX$  coded in XS-3, with digits  $\overline{NX}_i \in [-3, 12]$  and  $[\overline{NX}_i] = \overline{NX}_i + 3 \in [0, 15]$ .

#### 4.2 Most-Significant Digit Encoding

The MSD of each  $PP[k]$ ,  $PP_d[k]$ , is directly obtained in the ODDS representation. Note that these digits store the carries generated in the computation of the multiplicand multiples and the sign bit of the partial product. For positive partial products we have

$$PP_d[k] = T_{d-1} \quad (7)$$

with  $T_{d-1} \in \{0, 1, 2, 3, 4\}$  (see Table 2). For negative partial products, the ten's complement operation leads to

$$PP_d[k] = -10 + (9 - T_{d-1}) = -1 - T_{d-1} \quad (8)$$

with  $T_{d-1} \in \{0, 1, 2, 3, 4\}$ . Therefore the two cases can be expressed as

$$PP_d[k] = -Ys_k + (-1)^{Ys_k} T_{d-1}. \quad (9)$$

Since we need to encode  $PP_d[k]$  in the ODDS range  $[0, 15]$ , we add and subtract 8 in Eq. (9), resulting in

$$PP_d[k] = -8 + [PP_d[k]], \quad (10)$$

with

$$[PP_d[k]] = 8 - Ys_k + (-1)^{Ys_k} T_{d-1}.$$

Note that the term  $[PP_d[k]]$  is always positive. Specifically, for positive partial products ( $Ys_k = 0$ ), this term results in

TABLE 2  
Preferred Digit Recoding Mappings for  $NX$  Multiples

$X_i$	1X			2X			3X			4X			5X		
	$X_i + 3$	$T_i$	$D_i$	$(X_i \times 2) + 3$	$T_i$	$D_i$	$(X_i \times 3) + 3$	$T_i$	$D_i$	$(X_i \times 4) + 3$	$T_i$	$D_i$	$(X_i \times 5) + 3$	$T_i$	$D_i$
0	3	0	3	3	0	3	3	0	3	3	0	3	3	0	3
1	4	0	4	5	0	5	6	0	6	7	0	7	8	0	8
2	5	0	5	7	0	7	9	0	9	11	1	1	13	1	3
3	6	0	6	9	0	9	12	0	12	15	1	5	18	1	8
4	7	0	7	11	1	1	15	1	5	19	1	9	23	2	3
5	8	0	8	13	1	3	18	1	8	23	2	3	28	2	8
6	9	0	9	15	1	5	21	2	1	27	2	7	33	3	3
7	10	0	10	17	1	7	24	2	4	31	2	11	38	3	8
8	11	0	11	19	1	9	27	2	7	35	3	5	43	4	3
9	12	0	12	21	1	11	30	2	10	39	3	9	48	4	8

$8 + T_{d-1}$  that is within the range [8], [12] (since  $0 \leq T_{d-1} \leq 4$ ). For negative partial products ( $Y_{S_k} = 1$ ), this term results in  $7 - T_{d-1}$ , that is within the range [3], [7]. All of the  $-8$  terms of the different partial products are grouped together in a constant  $-8 \times \sum_{k=0}^{d-1} 10^{k+d}$  that is added as a constant correction term to the results of the reduction array.

Therefore, the  $PP_d[k]$ 's are encoded as  $[PP_d[k]]$  without the  $-8$  terms, which are added later (see Section 4.3), with only positive values of the form

$$[PP_d[k]] = \begin{cases} (8 + T_{d-1}), & \text{if } (Y_{S_k} = 0), \\ (7 - T_{d-1}), & \text{if } (Y_{S_k} = 1), \end{cases} \quad (11)$$

resulting in  $[PP_d[k]] \in [3, 12]$ .

This encoding is implemented at bit level as an inversion of the 3 LSB's of  $T_{d-1}$  if  $Y_{S_k} = 1$  and the concatenation of the MSB  $\bar{Y}_{S_k}$ .

### 4.3 Correction Term

The resultant partial product sum has to be corrected off-the-critical-path by adding a precomputed term,  $f_c(d)$ , which only depends on the format precision  $d$ . This term has to gather: (a) the  $-8$  constants that have not been included in the MSD encoding and (b) a  $-3$  constant for every XS-3 partial product digit (introduced to simplify the nine's complement operation).

Actually, the addition of these  $-3$  constants is equivalent to convert the XS-3 digits of the partial products to the ODDS representation. Note that the 4-bit encoding of a XS-3 digit  $NX_i$  (or  $9 - NX_i$ ) represents an ODDS digit with value  $[NX_i] = NX_i + 3 \in [0, 15]$  (or  $[9 - NX_i] = 15 - [NX_i] \in [0, 15]$ ).

The pre-computed correction term is given by

$$f_c(d) = -8 \times \sum_{k=0}^{d-1} 10^{k+d} - 3 \times \left( \sum_{i=0}^{d-1} (i+1)10^i + \sum_{i=0}^{d-2} (d-1-i)10^{i+d} \right). \quad (12)$$

Particularizing for  $d = 16$  and  $d = 34$  digit operands, the following expressions for the correction term in  $10$ 's complement are obtained:

$$\begin{aligned} f_c(16) &= -10^{32} + 07407407407407417037037037037037 \\ f_c(34) &= -10^{68} + 074074074074 \dots 07417037037037. \end{aligned} \quad (13)$$

The correction term is allocated into the array of  $d + 1$  partial products coded in ODDS (digits in  $[0, 15]$ ), as we show in the next section.

### 4.4 Partial Product Array

As a conclusion of the considerations in the previous sections, Fig. 4 illustrates the shape of the partial product array, particularizing for  $d = 16$ . Note that the maximum digit column height is  $d + 1$ .

In each column several components can be observed. Digits labeled with  $O$  represent the redundant excess-3 BCD digits in the set  $[0, 15]$ . Digits labeled with  $S_k$  represent the MSD of each partial product,  $PP_d[k]$  (see Section 4.2). The 16 least significant digits of the correction term  $f_c(16)$  are placed at the least significant position of each row after being added to  $Y_{S_k}$ , to complete the  $10$ 's complement in case of a negative partial product; thus  $H_k = Y_{S_k} + \{0, 3, 7\}$  (digitwise addition, out of the critical path), so that  $H_k \in [0, 8]$ . Note that the negative bit  $-10^{32}$  is canceled with the carry-out of the partial product sum in excess. The 16 leading digits of the correction term,  $[f_c(16)]_{dt}$ , are added to the most significant partial product  $PP[d]$ . Thus, in parallel with the evaluation of the multiplicand multiples we compute  $XF = X + [f_c(16)]_d$  in the ODDS representation (note that this computation does not involve a carry propagation and it is out of the critical path). Digits labeled as  $F$  in Fig. 4, represent the most-significant partial product,  $PP[d]$ , where  $PP[d] = XF$  if  $Y_{S_{d-1}} = 1$  and  $PP[d] = [f_c(16)]_d$  if  $Y_{S_{d-1}} = 0$ .

## 5 DECIMAL PARTIAL PRODUCT REDUCTION

The PPR tree consists of three parts: (1) a regular binary CSA tree to compute an estimation of the decimal partial product sum in a binary carry-save form ( $S, C$ ), (2) a sum correction block to count the carries generated between the digit columns, and (3) a decimal digit 3:2 compressor which increments the carry-save sum according to the carries count to obtain the final double-word product ( $A, B$ ),  $A$  being represented with excess-6 BCD digits and  $B$  being represented with BCD digits. The PPR tree can be viewed as adjacent columns of  $h$  ODDS digits each,  $h$  being the column height (see Fig. 4), and  $h \leq d + 1$ .

Fig. 5 shows the high-level architecture of a column of the PPR tree (the  $i$ th column) with  $h$  ODDS digits in  $[0, 15]$  (4 bits per digit). Each digit column of the binary CSA tree (the gray colored box in Fig. 5) reduces the  $h$  input digits and  $n_{cin}$  input carry bits, transferred from the previous

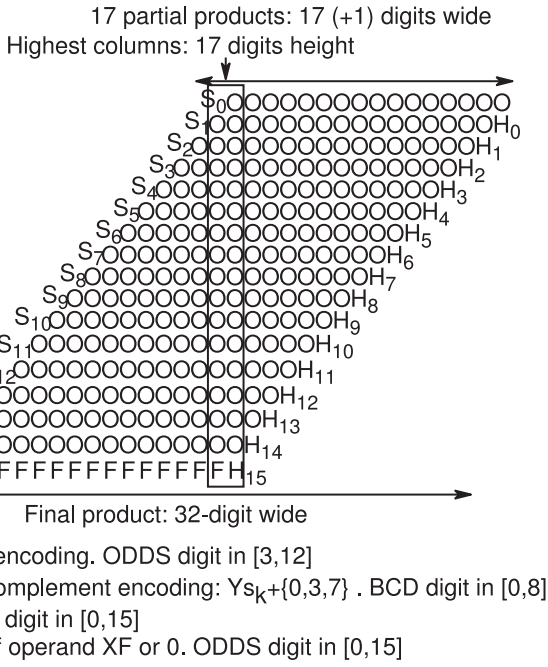


Fig. 4. Decimal partial product array generated for  $d = 16$  ( $16 \times 16$ -digit multiplier).

column of the binary CSA tree, to two digits,  $S_i$ ,  $C_i$ , with weight  $10^i$ . Moreover, a group of  $n_{cout}$  carry outputs are generated and transferred to the next digit column of the PPR tree. Roughly, the number of carries to the next column is  $n_{cout} = h - 2$ .

The digit columns of the binary CSA tree are implemented efficiently using 4-bit 3:2, 4:2 and higher order compressors made of full adders. These compressors take advantage of the delay difference of the inputs and of the sum and carry outputs of the full adders, allowing significant delay reductions.

The weight of the carry-outs generated at the  $i$ th column,  $c_{i+1}[0], \dots, c_{i+1}[n_{cout} - 1]$ , is  $16 \times 10^i$  because the addition of the 4-bit digits is modulo 16. These carries are transferred to the  $(i + 1)$ th column of the PPR tree, with weight  $10^{i+1} = 10 \times 10^i$ .

Thus, there is a difference between the value of the carry outs generated at the  $i$ -column and the value of the carries transferred to the  $(i + 1)$ -column. This difference,  $T$ , is computed in the sum correction block of every digit column and added to the partial product sum ( $S$ ,  $C$ ) in the decimal CSA.

Defining

$$W_i = \sum_{k=0}^{n_{cout}-1} c_{i+1}[k], \quad (14)$$

the contribution of the column  $i$  to the sum correction term  $T$  is given by

$$W_i \times 16 - W_i \times 10 = W_i \times 6. \quad (15)$$

Therefore, the sum correction is given by

$$T = \sum_{i=0}^{2d-1} (W_i \times 6 \times 10^i) = 6 \times \sum_{i=0}^{2d-1} W_i \times 10^i. \quad (16)$$

Consequently, the sum correction block evaluates  $W_i \times 6$ . This module is composed of a  $m$ -bit binary counter and a

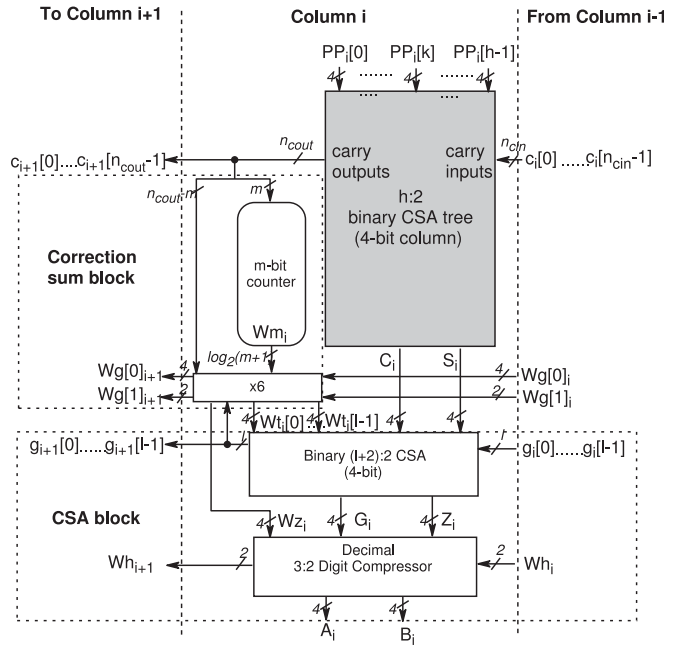


Fig. 5. High-level architecture of the proposed decimal PPR tree ( $h$  inputs, 1-digit column).

$\times 6$  operator. A straightforward implementation would use  $m = n_{cout}$  and a decomposition of the  $\times 6$  operator into  $\times 5$  and  $\times 1$  (both without long carry propagations), and then a four to two decimal reduction to add the correction to the PPR tree result.

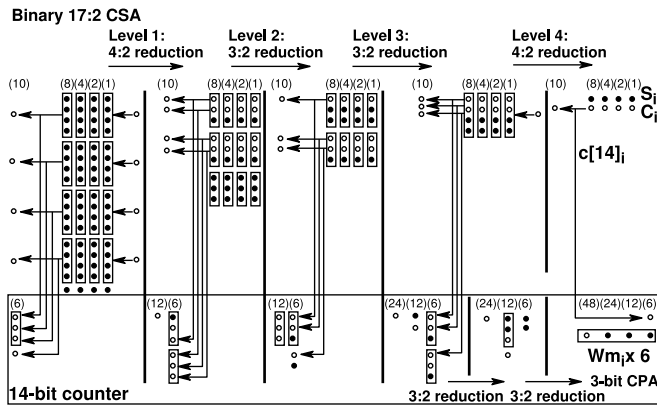
However, to balance paths and reduce the critical path delay we considered some optimizations. Specifically, the optimized implementation of this block heavily depends on the precision of the decimal representation; therefore its implementation is merely outlined here, without going into details. A detailed description of the implementation of the sum correction block is provided in Sections 5.1 and 5.2 for the Decimal64 and Decimal128 formats, respectively.

To obtain  $W_i$ , the carries generated in the column are split into two parts: the  $m$ -bit counter adds the  $m$  first carries of the binary digit column and produces a binary sum  $Wm_i$  of  $\lceil \log_2(m + 1) \rceil$  bits. The counter is implemented with full adders. To reduce the delay, the different arrival times of the carries have been taken into account.

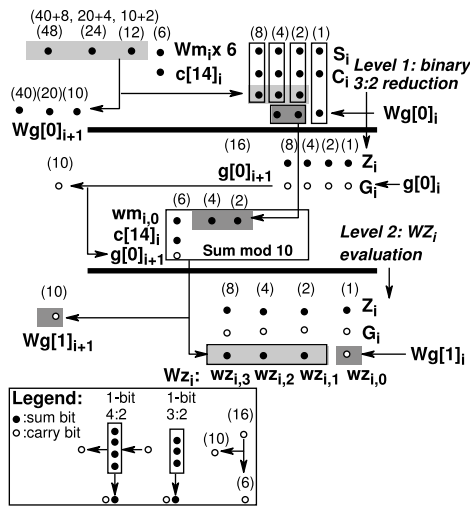
Fig. 6a shows the dot-diagram representation of this reduction for a digit column with  $h = 17$  (max. column height for Decimal64).

On the other hand, the remaining  $n_{cout} - m$  carries are introduced directly into the  $\times 6$  block. Note that a suitable value for  $m$  minimizes the delay overhead due to the sum correction and simplifies the logic of the  $\times 6$  operation. The best value for  $m$  depends basically on  $h$ , the height of the corresponding digit column. It was first estimated using the delay evaluation model described in Section 7.1 and then validated by automated RTL synthesis of the VHDL model.

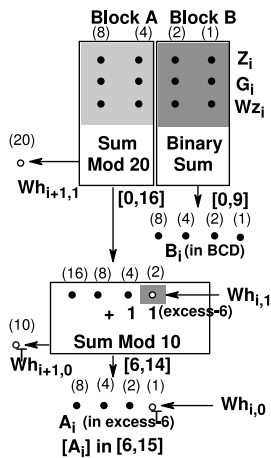
The low-level implementation details of the  $\times 6$  module depend on the number of carry-outs,  $n_{cout}$  and on the size of the counter,  $m$ , and are explained in Sections 5.1 and 5.2. However, it can be advanced that the  $\times 6$  operation generates at most two carry digits  $Wg[0]_{i+1}$ ,  $Wg[1]_{i+1}$  to the next column. Moreover, to illustrate the stage, we show the



(a) Stage 1. Binary 17:2 CSA and 14-bit counter.



(b) Stage 2. Decimal  $\times 6$  correction.



(c) Stage 3. Decimal 3:2.

Fig. 6. Dot-diagrams for the proposed decimal PPR ( $h = 17$  inputs, 1-digit column).

corresponding dot-diagram representation for  $h = 17$  ( $m = 14$ ) in Fig. 6b. An efficient implementation is obtained by representing the digit of  $W_i \times 6$  with  $l$  ODDS digits,  $Wt_i[0], \dots, Wt_i[l - 1]$ , being  $l = 1$  for Decimal64, and  $l = 2$  for Decimal128.

After that, the sum correction digits ( $Wt_i[0], \dots, Wt_i[l - 1]$ ) and the output digits of the binary CSA tree ( $S_i, C_i$ ) are

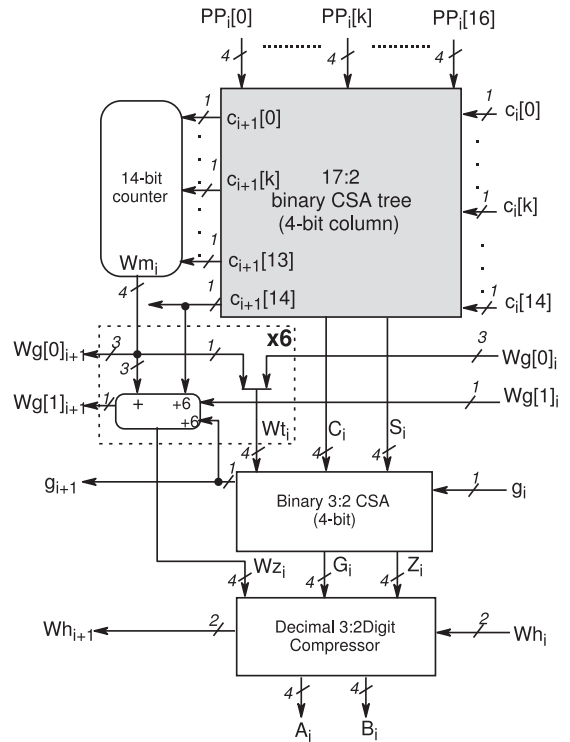


Fig. 7. Implementation of the PPR Tree Highest Column ( $h = 17$ ) for a  $16 \times 16$ -digit multiplication.

reduced to two ODDS digits  $G_i \in [0, 15]$ , and  $Z_i \in [0, 15]$ , using a 4-bit binary  $(l + 2) : 2$  CSA. This CSA generates  $l$  carry outs  $g_{i+1}[0], \dots, g_{i+1}[l - 1]$  with weight  $16 \times 10^i$ , which are transferred to the next column, and introduced into the  $\times 6$  block to produce another ODDS digit,  $Wz_i \in [0, 15]$ .

The last step is the addition of digits  $G_i, Z_i, Wz_i$  of the column,  $G_i + Z_i + Wz_i \in [0, 45]$ . We have designed a decimal 3:2 digit compressor that reduces digits  $Wz_i, G_i$  and  $Z_i$  to two digits  $A_i, B_i$ . The dot-diagram of the decimal 3:2 digit compressor is shown in Fig. 6c. To obtain the final BCD product by using a single BCD carry propagate addition, that is,  $P = A + B$ , which is the last step in the multiplication (see Fig. 1 and Section 3), it is required that  $A_i + B_i \in [0, 18]$ . Moreover, to reduce the delay of the final BCD carry-propagate adder (see Section 6) operand A is obtained in excess-6, so that we compute  $[A_i] = A_i + e$  in excess  $e = 6$  as defined by Equation (2), being the output digits sum  $[A_i] + B_i \in [6, 24]$ .

The evaluation is split in two parts:

Block A computes the sum of the two MSBS of the input digits (the bits with weights 8 and 4), and a two-bit carry input  $Wh_i \in \{0, 1, 2, 3\}$ . This sum is in  $[0, 39]$ . The outputs of this block are a BCD digit  $A_i$  in excess-6  $[A_i] \in [6, 15]$  and a two-bit decimal carry output  $Wh_{i+1} \in \{0, 1, 2, 3\}$  which is transferred to the next column (the  $i + 1$ th column). Note that the LSB of the carry output  $Wh_{i+1}$  depends on the MSB of the input carry  $Wh_i$ . However, there is no further carry propagation since the LSB of  $Wh_{i+1}$  is just the LSB of  $[A_{i+1}]$ , that is,  $[A_{i+1,0}]$ .

On the other hand, Block B implements the sum of the two LSB bits of the input digits (the bits with weights 2 and 1). This sum is in  $[0, 9]$ , so that  $B_i$  is evaluated as a regular binary addition.

## 5.1 Decimal 64 Implementation

The partial product array generated in the proposed  $16 \times 16$ -digit BCD multiplier is shown in Fig. 4. The maximum column height in the partial product array is  $h_{max} = d + 1 = 17$ . Therefore, a binary  $17 : 2$  CSA tree is required in this case, while other columns need CSA trees with a smaller number of inputs. Fig. 7 shows the implementation of the PPR tree for the maximum height columns. As stated previously, the maximum number of carries transferred between adjacent columns of the binary  $17 : 2$  CSA tree is 15. These carries are labeled  $c_{i+1}[0], \dots, c_{i+1}[14]$  (output carries) and  $c_i[0], \dots, c_i[14]$  (input carries) in the figure.

The binary  $17 : 2$  CSA tree is built of a first level composed of a  $9 : 2$  compressor and a  $8 : 2$  compressors, and a second level composed of a  $4 : 2$  compressor. To balance the delay of the  $17 : 2$  CSA tree and the bit counter,  $m = 14$  has been chosen.

The 14-bit counter produces the 4-bit digit  $Wm_i$ . The computation of  $Wm_i \times 6$  deserves a more detailed description. The 4-bit digit  $Wm_i = wm_{i,3}, wm_{i,2}, wm_{i,1}, wm_{i,0}$ , with  $wm_{i,j}$  being the bits of the digit, is conveniently represented as

$$Wm_i = Wg[0]_{i+1} \times 2 + wm_{i,0}, \quad (17)$$

with

$$Wg[0]_{i+1} = \sum_{j=1}^3 wm_{i,j} \times 2^{j-1}. \quad (18)$$

Note that  $Wm_i$  has been split into two parts, the three most-significant bits,  $Wg[0]_{i+1} \in [0, 7]$ , and the least-significant bit,  $wm_{i,0}$ . Then,  $W_i = Wm_i + c_{i+1}[14]$  results in

$$W_i = Wg[0]_{i+1} \times 2 + wm_{i,0} + c_{i+1}[14], \quad (19)$$

and consequently,

$$\begin{aligned} W_i \times 6 &= Wg[0]_{i+1} \times 12 + (wm_{i,0} + c_{i+1}[14]) \times 6 \\ &= (Wg[0]_{i+1} \times 10 + Wg[0]_{i+1} \times 2) \\ &\quad + (wm_{i,0} + c_{i+1}[14]) \times 6. \end{aligned} \quad (20)$$

The first term in Equation (20) represents a digit transfer to the next column. On the other hand, multiplication by 2 is implemented by shifting the binary representation of  $Wg[0]_{i+1}$  one bit to the left, so that  $Wg[0]_{i+1} \times 2 \in [0, 14]$  and its least-significant bit is 0.

Then, the sum correction term (*sct*) at the  $i$ th column, discarding the digit ( $Wg[0]_{i+1} \times 10$  transferred to the  $i + 1$ th column and taking into account the digit transferred from the  $i - 1$ th column, is given by

$$sct = Wg[0]_{i+1} \times 2 + (wm_{i,0} + c_{i+1}[14]) \times 6 + Wg[0]_i. \quad (21)$$

This sum correction term has been encoded in two ODDS digits  $Wt_i \in [0, 15]$  and  $Wz_i \in [0, 15]$  as follows

- Digit  $Wt_i$  is obtained by the concatenation of the most-significant bit of  $Wg[0]_{i+1} \times 2$  and  $Wg[0]_i$ , the digit transfer from the  $i - 1$ th column. Note that  $Wg[0]_i$  is represented with only three bits ( $Wg[0]_i \in [0, 7]$ ) and the concatenation of the most-significant digit of  $Wg[0]_{i+1} \times 2$  results in a 4-bit digit  $Wt_i \in [0, 15]$ .

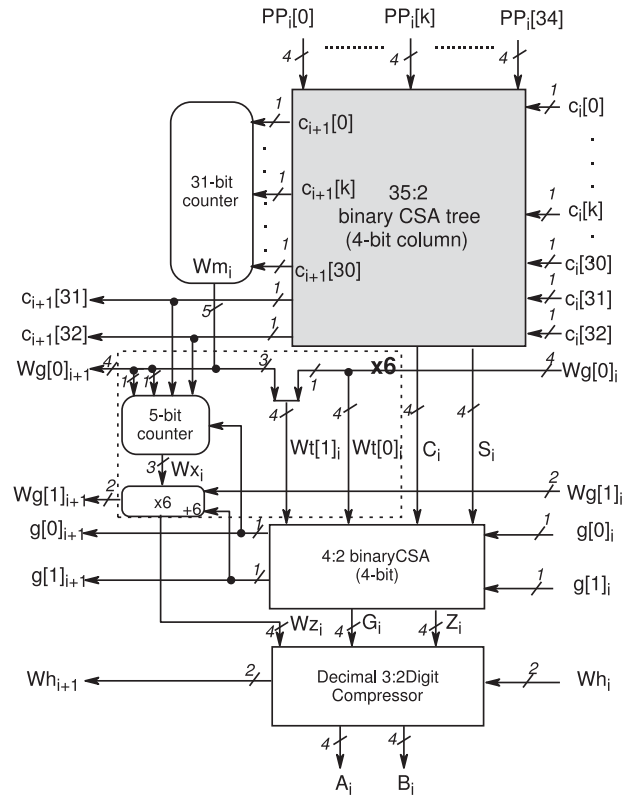


Fig. 8. Implementation of the PPR Tree Highest Column ( $h = 35$ ) for a  $34 \times 34$ -digit multiplication.

Digit  $Wt_i$  is added to the binary CSA tree column sum ( $S_i, C_i$ ) using a binary 4-bit  $3 : 2$  CSA, reducing these three digits to a double digit ( $G_i, Z_i$ ). A carry output  $g_{i+1}$  is transferred to the  $i + 1$ th column. Therefore, to obtain the sum correction term, the carry  $g_i$  transferred from  $i - 1$ th column has to be considered.

- Digit  $Wz_i$  is obtained by the addition of the two least significant bits of  $Wg[0]_{i+1} \times 2$ ,  $(wm_{i,0} + c_{i+1}[14]) \times 6$  (see Equation (21)) and the carry  $g_{i+1} \times 6$ . Moreover, this addition produces a carry out bit  $Wg[1]_{i+1}$  and a sum digit in  $[0, 14]$ . A carry-in  $Wg[1]_i$  is concatenated to this sum digit to obtain  $Wz_i$ .

Finally, a row of decimal  $3 : 2$  digit compressors is used to reduce the 3-operand partial product sum ( $G, Z, Wz$ ) to two BCD operands ( $A, B$ ), with  $A$  represented in excess-6 (see Fig. 6c).

## 5.2 Decimal 128 Implementation

The maximum height of the partial product array by the  $34 \times 34$ -digit BCD multiplier is  $h = 35$ . The proposed implementation for the maximum height columns of the PPR tree is shown in Fig. 8. The binary  $35 : 2$  CSA tree is built of a first level of three  $9 : 2$  and one  $8 : 2$  compressors, and a second level of one  $8 : 2$  compressor. The number of carries transferred to the next column of the binary CSA tree is 33.

The optimal value for parameter  $m$  is  $m = 31$ . Therefore, the addition of these carries has been split into two parts. First, a 31-bit counter evaluates  $Wm_i$ , the 5-bit sum of the 31 fastest carries. Then, the two slowest carries,  $c_{i+1}[31]$  and  $c_{i+1}[32]$ , are added to  $Wm_i$  into a second 5-bit counter.

TABLE 3  
Area and Delay Eqs. in the LE-Based Model [32]

Component	Delay (FO4)	$L_{in}$ (# inv)	Area (NAND2)
Nand2	0.4+ 0.2 $L_{out}$	4/3	1
Xor2	0.9+ 0.2 $L_{out}$	2	2.5
FA (sum, carry)	(2.2, 0.8)+ 0.2 $L_{out}$	5	10
Bin. 4:2 CSA	4.0+ 0.2 $L_{out}$	5	20
4-bit bin. CLA	4.5+ 0.2 $L_{out}$	5	45
BCD (4-bit) CLA	5.4+ 0.2 $L_{out}$	5	60

Operation  $Wm_i \times 6$  is decomposed as follows:

$$Wm_i \times 6 = Wg[0]_{i+1} \times 10 + Wg[0]_{j+1} \times 2 + wm_{i,0} \times 6 \quad (22)$$

with

$$Wg[0]_{i+1} = \sum_{j=1}^4 wm_{i,j} \times 2^{j-1} \in [0, 15].$$

As in the decimal 64 case, the first term is transferred to the  $i + 1$ th column and the multiplication by 2 is implemented as a one-bit binary left shift. The concatenation of digit  $Wg[0]_i$ , transferred from column  $i - 1$ , produces two redundant BCD digits  $Wt[0]_i \in [0, 15]$  and  $Wt[1]_i \in [0, 15]$ .

The 5-bit counter adds the remaining terms in Equation (22) with carries  $c_{i+1}$ [31] and  $c_{i+1}$ [32] and the multiplication  $\times 6$  produces a 4-bit digit  $Wz_i$  and two carries to the  $i + 1$ th column,  $Wg[1]_{i+1}$ .

After that, digits  $S_i, C_i, Wt[0]_i, Wt[1]_i$ , are reduced to two digits  $G_i, Z_i \in [0, 15]$  using a 4-bit binary 4 : 2 CSA. The two carries generated in the 4-bit 4 : 2 CSA are transferred to the next column  $i + 1$  and introduced into the 5-bit counter.

Finally, the three digits  $G_i, Z_i, Wz_i$  are reduced to two excess-6 BCD digits  $A_i$  and  $B_i$  by using the decimal digit 3 : 2 compressor.

## 6 FINAL CONVERSION TO BCD

The selected architecture is a  $2d$ -digit hybrid parallel prefix/carry-select adder, the BCD Quaternary Tree adder [29]. The delay of this adder is slightly higher to the delay of a binary adder of  $8d$  bits with a similar topology.

The decimal carries are computed using a carry prefix tree, while two conditional BCD digit sums are computed out of the critical path using 4-bit digit adders which implements  $[A_i] + B_i + 0$  and  $[A_i] + B_i + 1$ . These conditional sums correspond to each one of the carry input values. If the conditional carry out from a digit is one, the digit adder performs a  $-6$  subtraction. The selection of the appropriate conditional BCD digit sums is implemented with a final level of 2 : 1 multiplexers.

To design the carry prefix tree we analyzed the signal arrival profile from the PPRT tree, and considered the use of different prefix tree topologies to optimize the area for the minimum delay adder.

## 7 EVALUATION AND COMPARISON

The proposed combinational architectures for BCD  $16 \times 16$ -digit and  $34 \times 34$ -digit multipliers are evaluated and compared with other representative BCD multipliers. The area and delay figures of our architectures were obtained from an area-delay evaluation model for static CMOS gates, and validated with the synthesis of verified RTL models coded in VHDL. This evaluation is detailed in Section 7.1.

TABLE 4  
Area and Delay (LE-Based Model) for the Proposed Mults

Component	$16 \times 16$ -digit mult.		$34 \times 34$ -digit mult.	
	Delay #FO4	Area #NAND2	Delay #FO4	Area #NAND2
SD rec.+buff	7.0*	500	7.5*	1000
Multiples+buff.	5.9	1500	6.3	3100
Selection	3.2*	12900	3.2*	57500
PPG stage	10.2	14900	10.7	61600
PPR tree	25.5	11700	32.3	50000
Conversion	4.2	1600	4.2	3400
Decimal adder	11.5	2400	13.6	4600
Total stage	51.4	30600	60.8	119600

\*These terms contribute to the critical path delay.

Finally, the most representative sequential and parallel decimal multipliers have been compared with our architecture. The results of the comparison are summarized in Section 7.2.

### 7.1 Evaluation

As stated above, the evaluation has been performed in two steps. First, a technological independent evaluation using a model for static CMOS circuits based on Logical Effort (LE) [32] has been carried out, and then the results obtained with this model have been validated with the synthesis and functional verification of the RTL model.

#### 7.1.1 Technological Independent Evaluation

Our technological independent evaluation model [32] allows us to obtain a rough estimation of the area and delay figures for the architecture being evaluated. It takes into account the different input and output gate loads, but neither interconnections nor gate sizing optimizations are modeled. The delay is given in FO4 units, that is, the delay of an  $1 \times$  inverter with a fanout of four inverters. The hardware complexity is given as the number of equivalent minimum size NAND2 gates. We do not expect this rough model to give absolute area-delay figures, due to the high wiring complexity of parallel multipliers. However, based on our experience this model is good enough for making design decisions at gate level and it provides reasonable accuracy of area and delay ratios to compare different designs.

Table 3 shows the delay, input capacitance ( $L_{in}$ ) and area of the main building blocks used in the BCD multipliers. The input capacitance is normalized to the input capacitance of the  $1 \times$  inverter. The  $L_{out}$  parameter represents the normalized output load connected to the gate. The XOR2 gate is implemented with CMOS transmission gates.

To evaluate our architectures, gates with the drive strength of the minimum sized ( $1 \times$ ) inverter have been assumed, and buffers have been inserted to deal with high loads. The critical path delay in every stage of the multiplier has been estimated as the sum of the delays of the gates on this critical path. The area and delay figures obtained for the  $16 \times 16$ -digit and  $34 \times 34$ -digit architectures are shown in Table 4.

#### 7.1.2 Synthesis Results

The designs have been synthesized using Synopsys Design Compiler B-2012.09-SP3 and a 90 nm CMOS standard cell library [11]. The FO4 delay for this library is 49 ps under

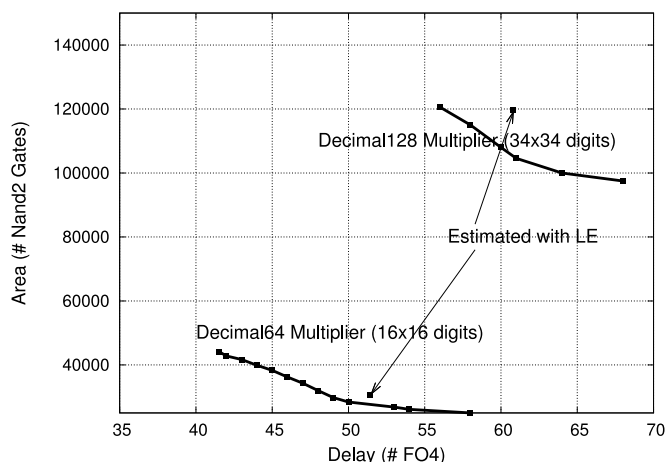


Fig. 9. Area-delay space obtained from synthesis.

typical conditions (1 V, 25° C). The area-delay curves of Fig. 9 have been obtained with the constraint  $C_{out} = C_{in} = 4C_{inv}$ , where  $C_{inv}$  is the input capacitance of a  $1\times$  inverter of the library.

We also include in Fig. 9 the area-delay points estimated from the LE-based model evaluation. We have kept the hierarchy of the design in the synthesis process as described in Sections 3 to 6 (no top level architecture optimization options). Nevertheless, some specific structures have been optimized internally to reduce the overall delay.

To ensure the correctness of the designs we have simulated the RTL models of the  $16\times 16$ -digit and  $34\times 34$ -digit multipliers using the Synopsys VCS-MX tool and a comprehensive set of random test vectors.

## 7.2 Comparison

Table 5 shows the area and delay estimations obtained from synthesis for some representative BCD sequential and combinational multipliers. As far as we know, the most representative high-performance BCD multipliers are  $16\times 16$ -digit combinational [12], [14], [16], [19], [30] and sequential [9], [10], [17] implementations. The area and delay figures shown

in Table 5 correspond to the minimum delay point of each implementation, and were obtained from the synthesis results provided in the respective reference, except for the two multipliers of reference [12], which correspond to an estimation obtained by their authors using a LE-based model. The comparison ratios are given with respect to the area and delay figures of a 53-bit binary Booth radix-4 multiplier extracted from [19].

The PPG of multipliers [7], [19] is based on a SD radix-5 scheme, that generates 32 BCD partial products for a 16-digit multiplier. Though it only requires simple constant time delay BCD multiplicand multiples, the 9's complement operation for obtaining the negative multiples is more complex than a simple bit inversion. The partial product reduction implemented in [19] is a BCD carry-save adder tree build of BCD digit adders. On the other hand, the BCD partial products are reduced in [7] by using counters that compute the binary sum of each column of digits sum, and subsequent binary to decimal conversions [7].

The BCD multiplier [16] pre-computes all the positive decimal multiplicand multiples  $\{0X, \dots, 9X\}$ . The delay of PPG is reduced by representing the complex operands  $\{3X, 6X, 7X, 8X, 9X\}$  as the sum of two simpler multiples. The number of partial products generated is therefore equivalent to that of the SD radix-5 scheme. The PPR tree is implemented with BCD digit adders as in [19]. This has the disadvantage of a large area compared to the other BCD multipliers analyzed.

The two  $16\times 16$ -digit BCD multipliers of [12] implement an easy-multiple PPG [9] (only precomputes  $\{2X, 4X, 5X\}$ ) that produces 32 BCD partial products. The intermediate decimal partial product sums are computed in overloaded BCD to speed up the PPR evaluation. The delay-improved design uses a tree structure built of five levels overloaded BCD digit adders, while the area-improved design replaces two levels of these custom designed adders by three levels of  $4:2$  compressors and a binary counter. This reduces the area consumption but at the cost of introducing a significant latency penalty.

TABLE 5  
Synthesis Results for Fixed-Point Multipliers

Architecture	Delay (# FO4)	Latency # Cycles	Latency (# FO4)	Ratio	Throughput Mult./Cycle	Area (NAND2)	Ratio
<b>Combinational multipliers:</b>							
Binary $53\times 53$ -bit:							
Booth radix-4	31.1	1	31.1	1.00	1	34000	1.00
BCD $16\times 16$ -digit:							
Ref. [19]	58.9	1	58.9	1.90	1	68000	2.00
Ref. [7]	55.8	1	55.8	1.80	1	68000	2.00
Ref. [16]	53.5	1	53.5	1.70	1	79600	2.35
Delay-Improved [12]	47	1	47	1.50	1	48600	1.45
Area-Improved [12]	51	1	51	1.65	1	39100	1.15
SD Radix-10 [30]	48	1	48	1.55	1	44500	1.30
SD Radix-5 [30]	46.5	1	46.5	1.50	1	49700	1.45
Ref. [14]	43.1	1	43.1	1.40	1	49900	1.45
Proposed	41.5	1	41.5	1.35	1	44200	1.30
BCD $34\times 34$ -digit:							
Proposed	56	1	56	1.80	1	120600	3.55
<b>Sequential multipliers (BCD <math>16\times 16</math>-digit):</b>							
Ref. [10]	16	20	320	10.20	1/17	16000	0.50
Ref. [9]	14.7	20	294	9.45	1/17	18550	0.55
Ref. [17]	12.7	24	305	9.80	1/17	31500	0.90

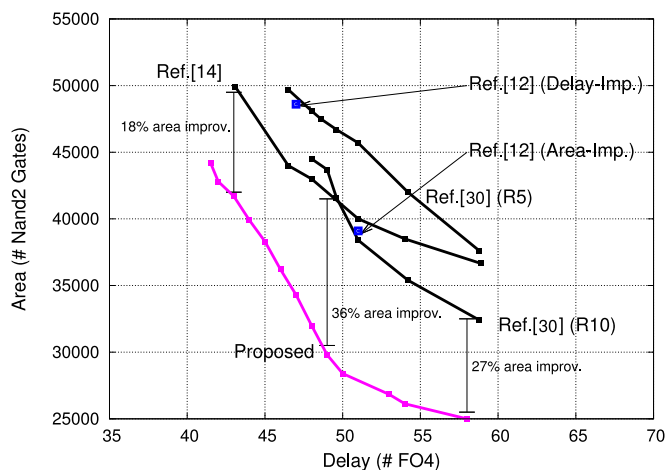


Fig. 10. Area-delay space for the fastest  $16 \times 16$ -digit multi.

The BCD multipliers in [30] use either the SD radix-5 PPG scheme or a SD radix-10 PPG scheme. The last one has the advantage that practically it halves the number of partial products generated by the former (17 against 32 for  $16 \times 16$ -digit multiplications). However, it has the disadvantage of a significant latency overhead due to the generation of the complex multiple  $3X$ . The latency and area of prior-art multipliers are improved by representing the partial products in (4221) or (5211) decimal codes, which allow them to implement PPR using a very regular and compact tree of 4-bit binary carry-save adders (built of  $3 : 2$  or  $4 : 2$  compressors) and decimal digit doublers.

The most recent implementation is presented in [14]. It also uses a SD radix-10 PPG scheme to reduce the number of partial products generated to 17, and subsequently, the area of the PPR tree. To avoid the latency overhead of the  $3 \times$  multiple generation, the partial products are coded in a redundant SD representation.

Sequential  $16 \times 16$ -digit (Decimal64) BCD multipliers are about two times smaller than equivalent parallel implementations, but have higher latency and reduced throughput (one mult issued every 17 cycles). For example, the proposed multiplier is about seven times faster than the best sequential implementation proposed in [9], but requires 2.5 times more area.

To compare the high hardware cost of a combinational Decimal128 implementation, we also include in Table 5 the area and delay figures obtained for our  $34 \times 34$ -digit BCD multiplier. Due to the tight area and power consumption constraints of current DFUs [5], a sequential architecture seems a more realistic solution than a fully pipelined implementation for a commercial Decimal128 multiplier.

Finally, we present a more detailed comparison of the fastest BCD  $16 \times 16$ -digit combinational multipliers (SD Radix-5 and SD Radix-10 [12], [14], [30], and the proposed one) in terms of latency and area. The corresponding area-delay synthesis values are shown in Fig. 10.

We have directly introduced in the figure the area-delay curves of referenced multipliers [30] and [14] as provided by their authors, since all of them were synthesized using 90 nm CMOS standard cell libraries and similar conditions. The area-delay points for the two multipliers of reference

[12] correspond to an estimation obtained by their authors using a LE-based model.

From the area-delay space represented in Fig. 10, we observe that our proposed decimal multiplier has an area improvement roughly in the range 20-35 percent depending on the target delay. On the other hand, for the minimum delay point ( $44FO4$ ), the proposed multiplier is still competitive with the fastest design shown in [14].

More recently, the authors of reference [12] have presented in [13] a comparison study between their delay-improved multiplier and the multiplier of reference [14] based on synthesis results using a TSMC 130 nm standard CMOS process under typical conditions (1.2 V,  $25^\circ$  C). They show that for the minimum delay point of each one of the two area-delay curves obtained, the delay-improved multiplier [12] is 20 percent faster and has 10 percent less area compared to the design of [14]. Therefore, according to [13] the curve corresponding to the design presented in [14] should be to the left of the area-delay points corresponding to the delay-improved design presented in [12].

## 8 CONCLUSION

In this paper we have presented the algorithm and architecture of a new BCD parallel multiplier. The improvements of the proposed architecture rely on the use of certain redundant BCD codes, the XS-3 and ODDS representations. Partial products can be generated very fast in the XS-3 representation using the SD radix-10 PPG scheme: positive multiplicand multiples (0X, 1X, 2X, 3X, 4X, 5X) are precomputed in a carry-free way, while negative multiples are obtained by bit inversion of the positive ones. On the other hand, recoding of XS-3 partial products to the ODDS representation is straightforward. The ODDS representation uses the redundant digit-set [0, 15] and a 4-bit binary encoding (BCD encoding), which allows the use of a binary carry-save adder tree to perform partial product reduction in a very efficient way. We have presented architectures for IEEE-754 formats, Decimal64 (16 precision digits) and Decimal128 (34 precision digits). The area and delay figures estimated from both a theoretical model and synthesis show that our BCD multiplier presents 20-35 percent less area than other designs for a given target delay.

## ACKNOWLEDGMENTS

Work supported in part by Ministry of Science and Innovation of Spain, co-funded by the European Regional Development Fund (ERDF/FEDER), under contract TIN2010-17541, and by the Xunta de Galicia under contracts 2010/28 and CN2012/151. The authors are members of the European Network of Excellence on High Performance and Embedded Architecture and Compilation (HiPEAC).

## REFERENCES

- [1] A. Aswal, M. G. Perumal, and G. N. S. Prasanna, "On basic financial decimal operations on binary machines," *IEEE Trans. Comput.*, vol. 61, no. 8, pp. 1084–1096, Aug. 2012.
- [2] M. F. Cowlishaw, E. M. Schwarz, R. M. Smith, and C. F. Webb, "A decimal floating-point specification," in *Proc. 15th IEEE Symp. Comput. Arithmetic*, Jun. 2001, pp. 147–154.
- [3] M. F. Cowlishaw, "Decimal floating-point: Algorithm for computers," in *Proc. 16th IEEE Symp. Comput. Arithmetic*, Jul. 2003, pp. 104–111.

- [4] S. Carlough and E. Schwarz, "Power6 decimal divide," in *Proc. 18th IEEE Symp. Appl.-Specific Syst., Arch., Process.*, Jul. 2007, pp. 128–133.
- [5] S. Carlough, S. Mueller, A. Collura, and M. Kroener, "The IBM zEnterprise-196 decimal floating point accelerator," in *Proc. 20th IEEE Symp. Comput. Arithmetic*, Jul. 2011, pp. 139–146.
- [6] L. Dadda, "Multioperand parallel decimal adder: A mixed binary and BCD approach," *IEEE Trans. Comput.*, vol. 56, no. 10, pp. 1320–1328, Oct. 2007.
- [7] L. Dadda and A. Nannarelli, "A variant of a Radix-10 combinational multiplier," in *Proc. IEEE Int. Symp. Circuits Syst.*, May 2008, pp. 3370–3373.
- [8] L. Eisen, J. W. Ward, H.-W. Tast, N. Mading, J. Leenstra, S. M. Mueller, C. Jacobi, J. Preiss, E. M. Schwarz, and S. R. Carlough, "IBM POWER6 accelerators: VMX and DFU," *IBM J. Res. Dev.*, vol. 51, no. 6, pp. 663–684, Nov. 2007.
- [9] M. A. Erle and M. J. Schulte, "Decimal multiplication via carry-save addition," in *Proc. IEEE Int. Conf. Appl.-Specific Syst., Arch., Process.*, Jun. 2003, pp. 348–358.
- [10] M. A. Erle, E. M. Schwarz, and M. J. Schulte, "Decimal multiplication with efficient partial product generation," in *Proc. 17th IEEE Symp. Comput. Arithmetic*, Jun. 2005, pp. 21–28.
- [11] *Faraday Tech. Corp.* (2004). 90nm UMC L90 standard performance low-K library (RVT). [Online]. Available: <http://freelibrary.faraday-tech.com/>
- [12] S. Gorgin and G. Jaberipur, "A fully redundant decimal adder and its application in parallel decimal multipliers," *Microelectron. J.*, vol. 40, no. 10, pp. 1471–1481, Oct. 2009.
- [13] S. Gorgin and G. Jaberipur. (2013, May). "High speed parallel decimal multiplication with redundant internal encodings," *IEEE Trans. Comput.* vol. 62, no. 5, [Online]. Available: <http://doi.ieee-computersociety.org/10.1109/TC.2013.160>
- [14] L. Han and S. Ko, "High speed parallel decimal multiplication with redundant internal encodings," *IEEE Trans. Comput.*, vol. 62, no. 5, pp. 956–968, May 2013.
- [15] *IEEE Standard for Floating-Point Arithmetic*, IEEE Std 754(TM)-2008 *IEEE Comput. Soc.*, Aug. 2008.
- [16] G. Jaberipur and A. Kaivani, "Improving the speed of parallel decimal multiplication," *IEEE Trans. Comput.*, vol. 58, no. 11, pp. 1539–1552, Nov. 2009.
- [17] R. D. Kenney, M. J. Schulte, and M. A. Erle, "High-frequency decimal multiplier," in *Proc. IEEE Int. Conf. Comput. Des.: VLSI Comput. Process.*, Oct. 2004, pp. 26–29.
- [18] R. D. Kenney and M. J. Schulte, "High-speed multioperand decimal adders," *IEEE Trans. Comput.*, vol. 54, no. 8, pp. 953–963, Aug. 2005.
- [19] T. Lang and A. Nannarelli, "A Radix-10 combinational multiplier," in *Proc. 40th Asilomar Conf. Signals, Syst., Comput.*, Oct. 2006, pp. 313–317.
- [20] T. Ohtsuki, Y. Oshima, S. Ishikawa, H. Yabe, and M. Fukuta, "Apparatus for decimal multiplication," U.S. Patent 4 677 583, Jun. 1987.
- [21] R. K. Richards, *Arithmetic Operations in Digital Computers*. New York, NY, USA: Van Nostrand, 1955.
- [22] M. Schmookler and A. Weinberger, "High speed decimal addition," *IEEE Trans. Comput.*, vol. C-20, no. 8, pp. 862–866, Aug. 1971.
- [23] E. M. Schwarz, J. S. Kapernick, and M. F. Cowlishaw, "Decimal floating-point support on the IBM System z10 processor," *IBM J. Res. Develop.*, vol. 51, no. 1, pp. 4:1–4:10, Jan./Feb. 2009.
- [24] B. Shirazi, D. Y. Y. Yun, and C. N. Zhang, "RBCD: Redundant binary coded decimal adder," *IEE Proc. E Comput. Digit. Techn.*, vol. 136, pp. 156–160, Mar. 1989.
- [25] H. Schmid, *Decimal Computation*. Hoboken, NJ, USA: Wiley, 1974.
- [26] T. Yoshida, T. Maruyama, Y. Akizuki, R. Kan, N. Kiyota, K. Ikenishi, S. Itou, T. Watahiki, H. Okano, "Sparc64 X: Fujitsu's new-generation 16-core processor for unix servers," *IEEE Micro.*, vol. 33, no. 6, pp. 16–24, Nov.-Dec. 2013.
- [27] A. Svoboda, "Decimal adder with signed digit arithmetic," *IEEE Trans. Comput.*, vol. C-18, no. 3, pp. 212–215, Mar. 1969.
- [28] C. Tsen, S. Gonzalez-Navarro, M. Schulte, B. Hickmann, and K. Compton, "A combined decimal and binary floating-point multiplier," in *Proc. 20th IEEE Int. Conf. Appl.-Specific Syst., Archit. Process.*, Jul. 2009, pp. 8–15.
- [29] A. Vazquez, E. Antelo, and P. Montuschi, "A new family of high-performance parallel decimal multipliers," in *Proc. 18th IEEE Symp. Comput. Arithmetic*, Jun. 2007, pp. 195–204.
- [30] A. Vazquez, E. Antelo, and P. Montuschi, "Improved design of high-performance parallel decimal multipliers," *IEEE Trans. Comput.*, vol. 59, no. 5, pp. 679–693, May 2010.

- [31] A. Vazquez and E. Antelo, "Multi-operand decimal addition by efficient reuse of a binary carry-save adder tree," in *Proc. 44th ASILOMAR Conf. Signals, Syst. Comput.*, Nov. 2010, pp. 1685–1689.
- [32] A. Vazquez and E. Antelo. (2012, Jun.). Area and Delay Evaluation Model for CMOS Circuits. Internal Report, Univ. of Santiago de Compostela, [Online]. Available: <http://www.ac.usc.es/node/1607>



**Alvaro Vazquez** received the graduation degree in physics in 1997, and the PhD degree in electronic and computer engineering from the University of Santiago de Compostela, Spain, in 2009. Currently, he is a postdoctoral researcher at the "Centro de Investigación en Tecnologías de la Información" (CITIUS), University of Santiago de Compostela. In 1998, he joined the Departamento de Electronica e Computacion at the University of Santiago de Compostela. He was a research visitor in the FPU Design Team at IBM R&D, Boeblingen, Germany, in 2008, for five months. From October 2009 to March 2011, he was an INRIA postdoc at the Laboratoire de l'Informatique du Parallelisme, ENS Lyon, France. His research interests are decimal floating-point arithmetic, design of high-speed and low-power numerical processors, FPGA-specific floating-point operators for reconfigurable computing, and algorithms and architectures for computing elementary functions. He is a member of the IEEE and the IEEE Computer Society.



**Elisardo Antelo** received the graduation degree in physics in 1991, and the PhD degree in computer engineering from the University of Santiago de Compostela, Spain, in 1995. In 1992, he joined the Departamento de Electronica e Computacion at the University of Santiago de Compostela. From 1992 to 1998, he was an assistant professor and, since 1998 he has been a tenured associate professor in this department. He was a research visitor at the University of California at Irvine several times between 1996 and 2000 and at the Politecnico di Torino in 2012. He is a member of the computer architecture group at the University of Santiago de Compostela. Since 2001, he has been involved in the program committee of the IEEE Symposium on Computer Arithmetic (program cochair in the 2011 edition). He also was involved with the program committees of the Real Numbers and Computers Conference and EUROSIPCO. He was an associate editor of the *IEEE Transactions on Computers* (2007–2012), and of *Integration, the VLSI Journal* (2011–2012). His primary research and teaching interest are in digital design and computer architecture with current emphasis on high-speed and low-power numerical processors, application-specific modules, computer arithmetic and design issues related to multicore processors.



**Javier D. Bruguera** received the graduation degree in physics, and the PhD degree from the University of Santiago de Compostela, Spain, in 1984 and 1989, respectively. Currently, he is a professor in the Department of Electronic and Computer Science at the University of Santiago de Compostela, Spain, and he is also with the "Centro de Investigación en Tecnologías de la Información" (CITIUS), University of Santiago de Compostela. Previously, he was an assistant professor at the University of Oviedo, Spain, from 1984 to 1986, and an assistant professor at the University of A Coruña, Spain, from 1987 to 1990. He served as a Chair of the Department between 2006 and 2010. He was a research visitor in the Application Center of Microelectronics at Siemens, Munich, Germany, in 1993, for five months, and in the Department of Electrical Engineering and Computer Science at the University of California at Irvine, from October 1993 to December 1994. His primary research interests are in the area of computer arithmetic, processor design, and computer architecture. He is author/coauthor of nearly 150 research papers on journals and conferences. He has served on program committees for several IEEE, ACM, and other meetings. He is a member of the IEEE, the IEEE Computer Society and ACM.

▷ For more information on this or any other computing topic, please visit our Digital Library at [www.computer.org/publications/dlib](http://www.computer.org/publications/dlib).